Low-temperature spin dynamics in the kagome system $Pr_3Ga_5SiO_{14}$

L. L. Lumata,[1,2] T Besara,[3,2] P. L. Kuhns,[2] A. P. Reyes,[2] H. D. Zhou,[1,2] C. R. Wiebe,[4,2,*] L. Balicas,[2] Y. J. Jo,[2] J. S. Brooks,[2] Y. Takano,[5] M. J. Case,[2] Y. Qiu,[6,7] J. R. D. Copley,[6] J. S. Gardner,[6,8] K. Y. Choi,[2] N. S. Dalal,[3,2] and M. J. R. Hoch[1,2]

[1]*Department of Physics, Florida State University, Tallahassee, Florida 32306-3016, USA*

[2]*National High Magnetic Field Laboratory, Florida State University, Tallahassee, Florida 32306-4005, USA*

[3]*Department of Chemistry, Florida State University, Tallahassee, Florida 32306-3016, USA*

[4]*Department of Chemistry, University of Winnipeg, Winnipeg, Manitoba, Canada R3B 2E9*

[5]*Department of Physics, University of Florida, Gainesville, Florida 32611, USA*

[6]*NIST Center for Neutron Research, Gaithersburg, Maryland 20899-6102, USA*

[7]*Department of Materials Science and Engineering, University of Maryland, College Park, Maryland 20742, USA*

[8]*Indiana University, 2401 Milo B. Sampson Lane, Bloomington, Indiana 47408, USA*

(Received 10 November 2008; revised manuscript received 6 May 2010; published 9 June 2010)

Neutron-scattering measurements on a single crystal of the distorted kagome system $Pr_3Ga_5SiO_{14}$ show that in zero magnetic field the system does not order magnetically at temperatures as low as 35 mK. The specific heat is found to exhibit T^2 behavior below 4 K. These results are indicative of a low-temperature two-dimensional dynamically disordered state in this geometrically frustrated antiferromagnet. Complementary in-field NMR experiments reveal that the spins remain dynamic down to millikelvin temperatures exhibiting spin-correlation times that are field dependent. The results are consistent with a field-dependent gap in the low-energy excitation spectrum. Diffuse neutron-scattering observations suggest that the application of a magnetic field induces dynamical short-range ordering.

DOI: 10.1103/PhysRevB.81.224416 PACS number(s): 75.25.−j, 78.70.Nx, 71.27.+a

I. INTRODUCTION

Two-dimensional (2D) triangular lattices, including kagome systems, exhibit intriguing low-temperature spin dynamics induced by a geometrical frustration.[1–16] The prototypical kagome examples are $ZnCu_3(OH)_6Cl_{12}$ [$Cu^{2+}(S=1/2)$], $SrCr_{8-x}Ga_{4+x}O_{19}$ [$Cr^{3+}(S=3/2)$], and the jarosite $(D_3O)Fe_3(SO_4)_2(OD)_6$ [$Fe^{3+}(S=5/2)$].[3–5] Systems of particular interest include the paratacamites $Zn_xCu_{4-x}(OH)_6Cl_{12}$,[3] which show a spin-liquid state. However, the 2D kagome lattice has proved to be difficult to synthesize and several of these materials have site disorder issues or are difficult to produce in single-crystalline form.[4] The above examples are all 3*d* transition-metal-based compounds in which the exchange interactions and geometrical frustration are of dominant importance while Dzyaloshinsky-Moriya interactions, single-ion anisotropies, and off-stoichiometry serve as perturbations. Investigation of the predicted spin-liquid state is complicated by the presence of these perturbations.

For rare-earth (RE) compounds, the situation is somewhat different to that found in the 3*d* transition-metal cases. Specifically, for the rare-earth cases the single-ion anisotropies govern the overall magnetic behavior while frustration-induced spin dynamics is expected to emerge at energies well below the crystal-field splitting between the ground state and the first excited state. It is therefore of considerable interest that the recently discovered RE-based kagome compounds $R_3Ga_5SiO_{14}$ (R=Nd or Pr) show a disordered state at low temperatures.[17–20] The cooperative magnetic correlations depend on the RE ion involved and the crystal-field environment. We have addressed this issue by studying the spin dynamics of the RE kagome non-Kramers ion $Pr_3Ga_5SiO_{14}$ system and making comparisons to the behavior of its sister isostructural Kramers ion counterpart $Nd_3Ga_5SiO_{14}$ which has different magnetocrystalline anisotropy.[19,20]

$Pr_3Ga_5SiO_{14}$, which belongs to the langasite family, has a trigonal crystal structure with the RE Pr^{3+} ions ($5f^2$:J=4) networked as corner-sharing triangles to form a distorted kagome-type lattice (see Fig. 1). At high temperatures the magnetic susceptibility χ obeys the Curie-Weiss law consistent with antiferromagnetic (AF) correlations between the Pr^{3+} spins.[18]

Muon spin-relaxation (μSR) and NMR measurements on $Nd_3Ga_5SiO_{14}$ reveal that a disordered state persists down to low T in zero field.[18,19] Spin fluctuations are suppressed by an applied field and for H=0.5 T a field-induced transition is found at 60 mK. Although the two isostructural compounds $R_3Ga_5SiO_{14}$ (R=Pr^{3+} or Nd^{3+}) share, to some extent, common physics, detailed cooperative spin dynamics varies with the RE ions. This is because Pr^{3+} and Nd^{3+} have different crystal-field splittings, single-ion anisotropies, and exchange interactions leading to a substantial difference in low-energy spin dynamics, both at zero field and in an applied field.

In this paper, we report on the investigation of a single crystal of the distorted kagome system $Pr_3Ga_5SiO_{14}$ using magnetic susceptibility, specific heat, neutron scattering, and NMR. Taken together, the experimental results provide compelling evidence for a dynamical disordered state persisting to temperatures well below 1 K. Zorko *et al.*[19] have very recently made low-temperature zero-field muon spin-relaxation and nuclear quadrupole resonance (NQR) measurements of $Pr_3Ga_5SiO_{14}$. The results are interpreted in terms of a single-ion model with crystal-field splitting of the Pr^{3+} states and it is concluded that the system is a Van Vleck paramagnet with a nonmagnetic singlet ground state and a low lying excited state above the ground state. We have ad-

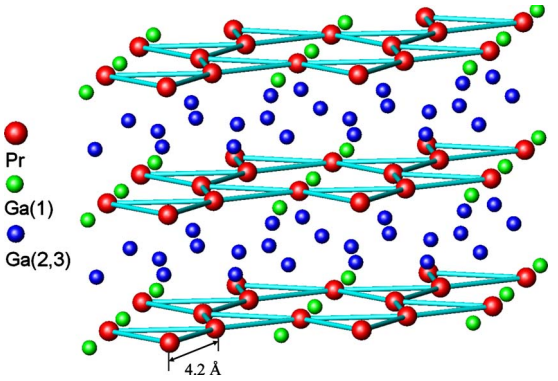

FIG. 1. (Color online) The crystal structure showing three distorted kagome planes of Pr^{3+} ions in the *ab* plane of $Pr_3Ga_5SiO_{14}$. Ga(2,3) sites lie between these planes and Ga(1) is in plane (see text).

dressed these claims in the present work with numerous sample property measurements and interpretation based on our results.

II. EXPERIMENTAL DETAILS AND RESULTS

Crystal growth and magnetic susceptibility

A single crystal of $Pr_3Ga_5SiO_{14}$ was grown by the traveling-solvent floating-zone technique. The room-temperature crystal structure was confirmed using an x-ray diffractometer equipped with Cu $K\alpha 1$ radiation. X-ray Laue diffraction was used to orient the crystal. $Pr_3Ga_5SiO_{14}$ crystallizes in the trigonal space group $P321$ with lattice parameters $a=8.0661(2)$ Å and $c=5.0620(2)$ Å (Fig. 2). The Pr^{3+} magnetic ions in $Pr_3Ga_5SiO_{14}$ are organized in corner-sharing triangles in well-separated planes perpendicular to the *c* axis. Within each plane, the Pr^{3+} ions form a distorted kagome lattice (Fig. 1), which is topologically equivalent to the ideal kagome when only the shortest atom bridging interactions are considered. The nearest Pr-Pr separation in the *ab* plane is 4.2 Å (Fig. 1). The atomic positions are listed in Table I.

The susceptibility was measured as a function of temperature using a dc superconducting quantum interference device magnetometer while heating the sample in a field of 1 T

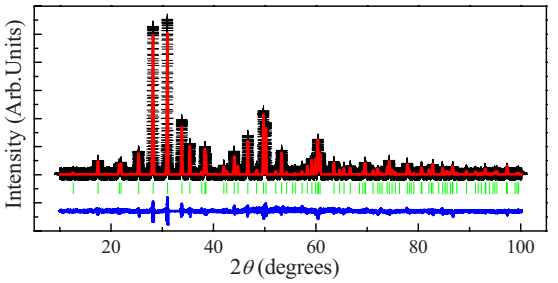

FIG. 2. (Color online) X-ray diffraction pattern for $Pr_3Ga_5SiO_{14}$ (plus marks) at room temperature. The solid curve is the best fit from the Rietveld refinement using FULLPROF. The vertical marks indicate the position of Bragg peaks, and the bottom curve shows the difference between observed and calculated intensities.

TABLE I. Crystallographic parameters at room temperature for $Pr_3Ga_5SiO_{14}$.

Site	*x*	*y*	*z*	*B* (Å^2)
Pr 3*e*	0.4185(2)	0	0	1.56(4)
Ga(1) 1*a*	0	0	0	1.62(4)
Ga(2) 3*f*	0.7648(6)	0	0.5	1.84(3)
Ga(3) 1*d*	1/3	2/3	0.5348(8)	1.87(6)
Si 1*d*	1/3	2/3	0.5348(8)	1.97(6)
O1 2*d*	2/3	1/3	0.8043(43)	2.15(3)
O2 6*g*	0.5343(27)	0.8524(34)	0.6912(35)	2.20(2)
O3 6*g*	0.2236(22)	0.0772(20)	0.7615(30)	2.15(2)

directed along the *c* axis, following cooling in zero field. Figure 3 shows the temperature dependencies of the dc magnetic susceptibility $[\chi(T)]$ and its inverse $[\chi^{-1}(T)]$. The results are similar to those obtained for this field orientation by Bordet *et al.*[17] The susceptibility above 50 K follows the Curie-Weiss law: $\chi^{-1}(T)=(T-\theta_{CW})/C$. The effective moment $\mu_{eff}=3.2(1)\mu_B$ calculated from the Curie constant *C* is smaller than that of a single Pr^{3+} ion ($\mu_{eff}=3.6\mu_B$), which is common for magnetically frustrated systems.[21] A small negative value for θ_{CW} is suggested by Fig. 3, consistent with the conclusion reached in Ref. 17. No magnetic anomalies in the dc susceptibility data were observed down to 1.8 K. In particular, no evidence for Van Vleck temperature-independent magnetism was found in the 1 T measurements at the lowest temperatures at which measurements were made.

To obtain information on the spin dynamics at low temperatures, ac susceptibility measurements were made on the single crystal with applied field parallel to the *c* axis. The ac susceptibility [Figs. 4(a) and 4(b)] shows no anomaly, nor any frequency dependence down to 1.8 K, which indicates that the characteristic spin-fluctuation rate is beyond the kilohertz region. The featureless ac susceptibility data exclude the possibility that $Pr_3Ga_5SiO_{14}$ is a spin glass at low temperatures.

III. SPECIFIC HEAT

The specific-heat measurements were made on a single crystal with an applied field parallel to the *c* axis. A dilution

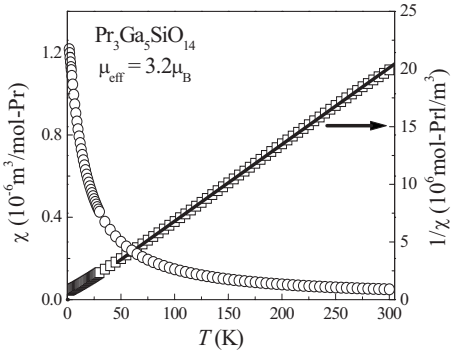

FIG. 3. Temperature dependencies of the powder dc susceptibility and its inverse.

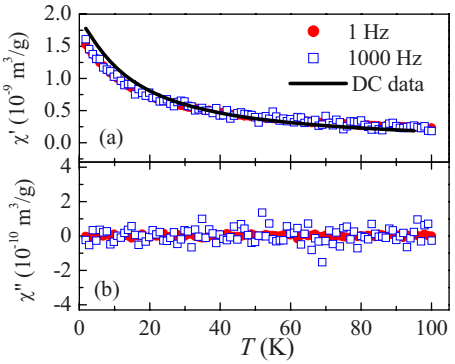

FIG. 4. (Color online) Temperature dependencies of the powder ac and dc susceptibility: (a) real part of ac response (in good agreement with the dc response) and (b) imaginary part of ac response at $f=1$ and 1000 Hz.

fridge was used to collect specific-heat data from 0.1 to 0.4 K. The results are shown as $C_P(T)/T$ in Fig. 5(a) and as $C_{mag}(T)/T$ in Fig. 5(b). The data show no evidence of a phase transition down to 0.1 K in zero field. The *magnetic* specific heat $C_{mag}(T)$ was estimated by subtracting the lattice contribution using $C_P(T)$ of $La_3Ga_5SiO_{14}$ with no magnetic ions as a reference. As shown in Fig. 5(b) $C_{mag}(T)/T$ exhibits a broad peak at $T_{peak}=6.7$ K. Another noteworthy feature is that below 0.3 K, the zero-field specific heat starts to increase with decreasing temperature [Fig. 6(a)]. This behavior suggests a nuclear Schottky anomaly at low temperatures with a maximum in C_P below 0.1 K. Higher field measurements made down to 1 K show a field-dependent shift in the specific heat, which is consistent with a low-T nuclear contribution. We cannot rule out the possibility of an electronic origin to this peak (as seen, from, for example, two closely spaced singlets or an electronic glass state such as mentioned by Zorko[19]), but given the nuclear energy level scheme of Pr, it is likely nuclear in origin.

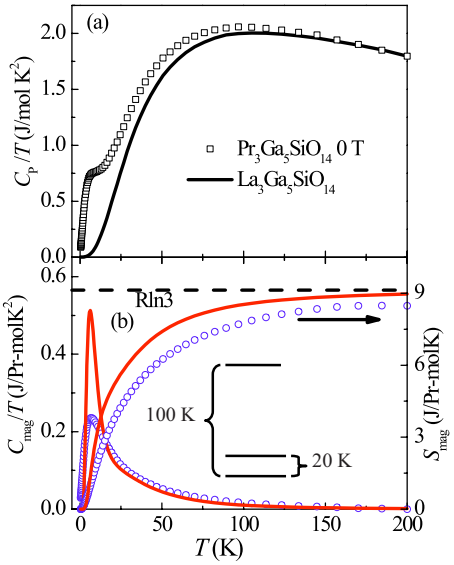

FIG. 5. (Color online) (a) Temperature dependencies of C_P/T for $Pr_3Ga_5SiO_{14}$ and $La_3Ga_5SiO_{14}$. (b) Temperature dependencies of C_{mag}/T for $Pr_3Ga_5SiO_{14}$. A fit is shown for a three-level crystal-field scheme as indicated.

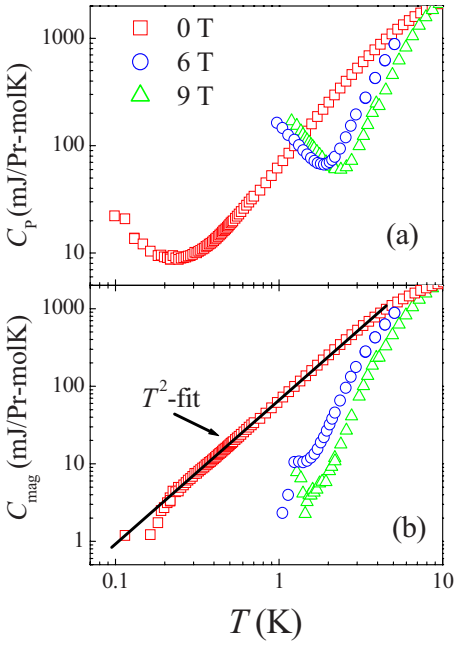

FIG. 6. (Color online) (a) Temperature dependencies of the specific heat at low temperatures for $Pr_3Ga_5SiO_{14}$ with applied fields of 0, 6, and 9 T along the c axis. (b) Magnetic contribution of specific heat after subtracting the Schottky anomaly and lattice contribution.

IV. NEUTRON SCATTERING

Neutron-scattering measurements were carried out at the NIST CHRNS facility using the disk chopper spectrometer (DCS) with a wavelength of 4.8 Å. The crystal (total mass of 5 g) was aligned in the ab plane with a vertical magnetic field applied in the c direction. A dilution fridge with a base temperature of 0.035 K was used for these experiments.

Figure 7(a) shows the elastic neutron-diffraction patterns at different temperatures and applied magnetic fields. No magnetic Bragg peaks are found down to 0.035 K in zero field, giving an upper bound of $0.05\mu_B$ for a possible ordered moment along the c axis within the resolution of our instrument. A caveat is needed here, however, since these scans are taken within the $[H,K,0]$ plane, and although they are integrated over upper and lower detectors which allows for some component along L, we cannot rule out an ordering wave vector of the form $[0,0,L]$, for example. Note that assuming there is no long-ranged ordering, this upper bound on the ordering temperature suggests a high value for the frustration index $f\sim|\theta_{CW}|/T_C$. Figure 7(b) shows integrated inelastic neutron scans, integrated over Q in the $[H,K,0]$ plane, as a function of applied field at 0.035 K. Note that at zero field there is a broad peak at $E=1.2$ meV$\sim$13 K. This excitation is clearly suppressed by applied fields.

Figure 8 shows the elastic neutron scattering ($-0.02<\hbar\omega<0.02$ meV) within the $[H,K,0]$ plane at 0.035 K with $H=9$ T. By masking the central bank [Fig. 8(b)], the data show clear diffuse scattering around the Bragg peaks, such as the (0,1,0) and (1,0,0) peaks. The central bank of the DCS is located 4.00 m from the sample and is 400 mm in length. In terms of scattering angle, the bank covers $-30°$ to $-5°$ and $+5°$ to $+140°$ within the scattering plane and $\pm2.9°$

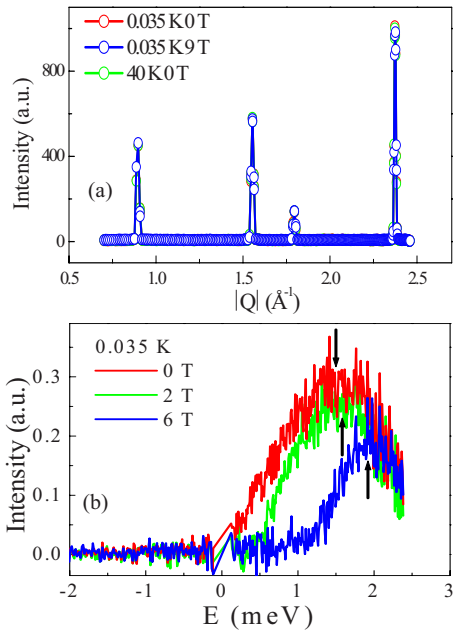

FIG. 7. (Color online) (a) Neutron-diffraction patterns at $T=0.035$ K, (0 T); $T=0.035$ K (9 T); and $T=40$ K, $H=0$ T show no magnetic Bragg peaks. (b) Inelastic neutron scattering integrated over Q in the $[H,K,0]$ plane at 0.035 K as a function of magnetic field along the c axis. The arrows indicate the peaks' positions.

out of the plane. By masking upper and lower banks [Fig. 8(a)], the data still show diffuse scattering with weaker intensity. The integrated diffuse neutron scattering results around the (0,1,0) peak obtained by masking the central bank at 0.035 K are given as a function of field in Fig. 9(a) while Fig. 9(b) shows the difference between patterns taken at $H=6$ and 9 T and that taken at $H=0$ T. With increasing field the intensity of the diffuse scattering increases and the peak broadens.

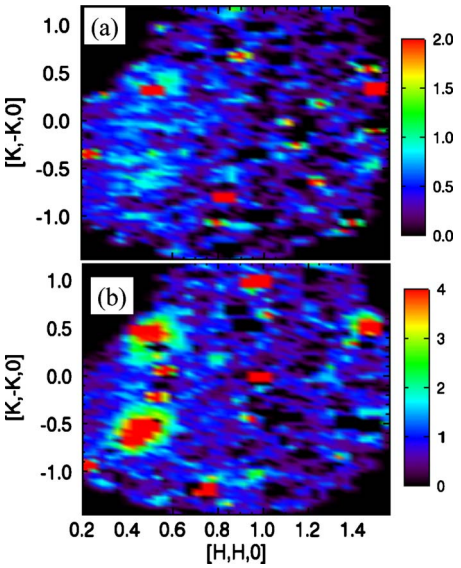

FIG. 8. (Color online) Elastic neutron scattering $(-0.02<\hbar\omega<0.02$ meV) within the $[H,K,0]$ plane at 0.035 K with $H=9$ T. (a) Masking the central bank (see text); (b) masking upper and lower banks.

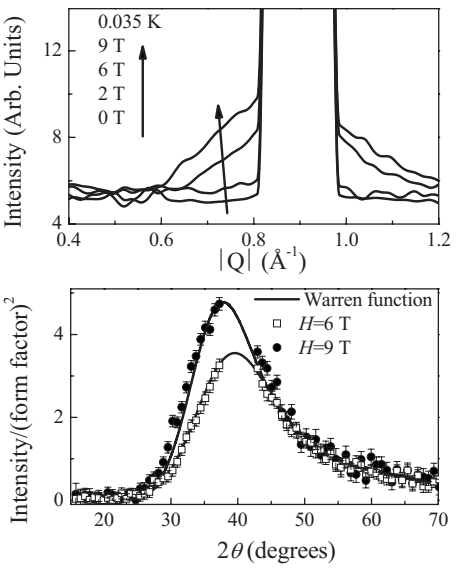

FIG. 9. (a) Integrated diffuse scattering around the (0,1,0) peak, with $-0.6<K<-0.4$ as shown in Fig. 8(b), by masking the central bank at 0.035 K as a function of magnetic field applied along the c axis. (b) Difference between patterns taken at $H=6$ and 9 T and that taken at $H=0$ T. The solid lines are fits to Eq. (1).

V. NMR SPECTRA AND RELAXATION RATES

The dynamically disordered ground state of $Pr_3Ga_5SiO_{14}$ suggested by the low-temperature neutron scattering makes this system particularly interesting for low-temperature NMR experiments. ^{69,71}Ga NMR spectra and relaxation rates were obtained using a computer-controlled pulsed spectrometer with sweepable superconducting magnet. A helium-3 cryostat was used for the measurements below 1 K. Figure 10 shows the field-swept spectra obtained by integrating ^{69,71}Ga spin-echo signals. Multiple peaks are found corresponding to three nonequivalent sites for the $I=3/2$ ^{69}Ga and

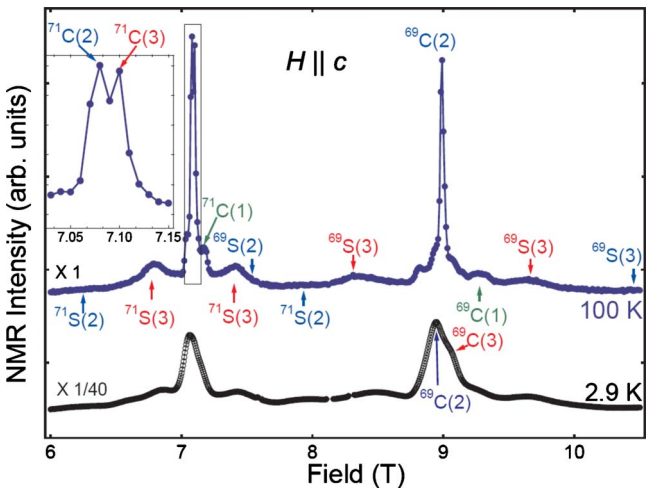

FIG. 10. (Color online) NMR field-scan spectra of $Pr_3Ga_5SiO_{14}$ at 92 MHz showing quadrupolar split ^{69}Ga ($I=3/2$) and ^{71}Ga ($I=3/2$) components for the three nonequivalent Ga sites. Resolved peaks are labeled central (C) or satellite (S) components. The left inset highlights the two ^{71}Ga central lines C(2) and C(3).

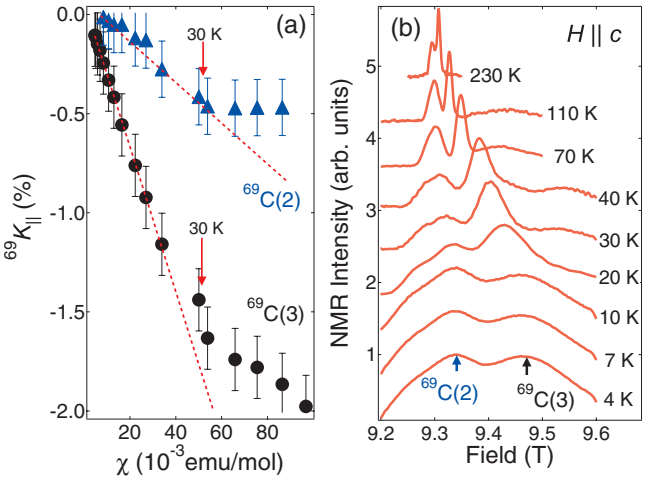

FIG. 11. (Color online) (a) ^{69}Ga NMR shifts measured in an applied field of 9 T along the crystal c axis plotted versus the magnetic susceptibility at 1 T with temperature as the implicit parameter. The plot shows a change in slope at $T \approx 30$ K. (b) ^{69}Ga field-swept NMR spectra at 95 MHz as a function of T.

^{71}Ga isotopes each having quadrupolar splittings which give rise to a central (C) line and two satellites (S) due to noncubic site symmetry. The resulting spectrum consisting of eighteen overlapping lines is similar to that of $Nd_3Ga_5SiO_{14}$,[19] except that the site assignments are different. From intensity arguments, we assign the double peak structure as the out-of-plane Ga(2,3) and the off-center weak signal as the in-plane Ga(1) site. The spin-lattice-relaxation rates at the Ga(2,3) sites are very similar. The principal components of the spectrum are denoted as C(2) and C(3) for each isotope. Figure 1 depicts the crystal structure showing three kagome planes with details of the three Ga sites.

Figure 11(a) plots the measured spectral NMR shift ^{69}K for $H=9$ T along c versus the bulk susceptibility $\chi_{||}$ with T as the implicit parameter while Fig. 11(b) shows the spectra in a stacked plot. The linewidth increases significantly as T is lowered below 100 K. For $T>30$ K a linear relationship between ^{69}K and $\chi_{||}$ is found, but the slope becomes less steep for $T<30$ K. In this low-temperature range the Pr^{3+} ions are increasingly occupying the ground state as the temperature is decreased. The interesting change in slope of the $\chi_{||}$ vs ^{69}K plot can be attributed either to a change in the hyperfine coupling due to the growing importance of AF correlations or to the local susceptibility differing from the bulk susceptibility.

In order to study the Pr^{3+}-ion spin dynamics as sensed at the Ga sites, spin-lattice $(1/T_1)$ and spin-spin $(1/T_2)$ relaxation rates were measured as functions of temperature for the central ^{69}Ga spectral component corresponding to ^{69}C(2) [see Fig. 11(b)]. Relaxation-rate measurements were made in several different applied magnetic fields directed parallel to the c axis and the results are given in Fig. 12. Similar results were found for the other spectral components. The behavior of the magnetic specific heat divided by T is shown for comparison and the temperature dependencies of $1/T_2$ and C_{mag}/T are similar. The ^{69}Ga magnetization recovery curves at low T could be fit using the master equation for a spin $I=3/2$ system $M=M_0[1-0.4\exp(-t/T_1)-0.6\exp(-6t/T_1)]$. Saturation of the central component was achieved using a comb of $\pi/2$ pulses. At low temperatures, where the linewidth becomes large and spectral components overlap it is not clear that the master equation approach remains valid. It was found that the data could be fit with a stretched exponential form $M=M_0[1-\exp(-t/T_1)^{\beta}]$ with stretch exponent $\beta=0.7$. The relaxation rate obtained using a single exponential in this temperature range gave values very similar to those from the stretched exponential fit. The $1/T_1$ values in the figure correspond to the stretched exponential form at low temperatures.

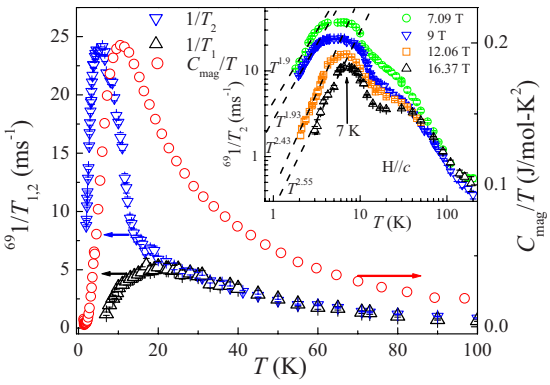

FIG. 12. (Color online) ^{69}Ga $1/T_1$ and $1/T_2$ for $Pr_3Ga_5SiO_{14}$ as a function of T at 9 T, together with magnetic specific heat divided by T at 9 T. Inset: log-log plot of $^{69}1/T_2$ at different fields. Below the peak a power-law behavior close to T^2 is observed as shown by the dashed lines.

The ^{69}Ga NMR signal in $Pr_3Ga_5SiO_{14}$ could be observed in all applied fields over the temperature range 0.3–290 K. This behavior contrasts with that found in the sister compound $Nd_3Ga_5SiO_{14}$ (Ref. 19) and other frustrated 2D antiferromagnets such as $NiGa_2S_4$ (Ref. 14) where NMR signal wipe-out occurs at low temperatures when (T_2) becomes very short.

Spin-lattice relaxation is attributed to fluctuating hyperfine fields, produced by the electron moments on nearby Pr^{3+} ions, which induce nuclear spin state transitions. Because of the compact $4f$ wave function, the fluctuating local field H_L which may be written as $H_L=H_{iso}+H_{aniso}$ has H_{aniso} at a Ga nuclear site primarily due to dipolar coupling between the electron S spin and the nuclear I spin. H_{iso} is the somewhat smaller transferred hyperfine interaction which is expected to play a minor role in the relaxation process. The dipolar coupling can induce an I spin flip without a corresponding S spin flip and produces a maximum in the relaxation rate when the correlation time is equal to the inverse of the nuclear Larmor frequency rather than the inverse of the S frequency that would apply for the transferred hyperfine coupling.[22,23]

VI. DISCUSSION

$Pr_3Ga_5SiO_{14}$ is a non-Kramers ion with $J=4$. Crystal-field interactions result in nine singlet states for this ion although accidental degeneracies, or near-degeneracies, may occur. A crystal-field calculation for $Pr_3Ga_5SiO_{14}$ has been carried out

in the high-temperature approximation in Ref. 17. The results are used to discuss the inverse susceptibility data but this approach provides only qualitative information because the measurements were not made at sufficiently high temperatures. More complete results have been obtained for the Kramers ion $Nd_3Ga_5SiO_{14}$ system as presented in Refs. 17, 20, and 24. The primary interest of the present work concerns the low-temperature dynamical properties of $Pr_3Ga_5SiO_{14}$. These properties are linked to low-energy states of the Pr^{3+} ions with allowance for interactions between spins. We have not attempted to extend the crystal-field calculation of Ref. 17, in part, because of the lack of sufficient number of experimental constraints that are required to fix the numerous coefficients involved. In addition, specific-heat calculations that we have carried out to fit the data, using various *ad hoc* models of discrete crystal-field states, do not reproduce the form of the measured magnetic specific-heat curve. One can obtain qualitatively similar behavior (see Fig. 5 with a singlet ground-state fit) but a single-ion picture clearly cannot reproduce the data. A full treatment of the energy states, allowing for interactions between spins at low temperatures, is expected to result in a density of states description rather than discrete crystal-field states. This conclusion is supported by the present neutron-scattering measurements. Nevertheless, features of the crystal-field split states are likely to be preserved. In particular, the magnetic-susceptibility data are consistent with a magnetic ground state which, in the single-ion limit, corresponds to a pair of degenerate or near-degenerate singlets.

The low-temperature Schottky upturn in the specific heat can be fit with a T^{-2} term. After correcting for this anomaly and the lattice contribution, the magnetic contribution to the low-T specific heat at zero field exhibits power-law behavior [Fig. 6(b)]. The zero-field data between 0.1 and 4 K are well fit by a power law $C_{\mathrm{mag}}=AT^{\alpha}$, where A is a constant and $\alpha=1.98(2)$. 2D spin excitations would give $C\sim T^2$. This quadratic temperature dependence without long-range magnetic order suggests the presence of linear modes in 2D, similar to other 2D kagome systems such as SCGO.[4]

In general, a peak at low temperature in $C(T)/T$ results from a peak in the density of states, $g(w)$, defined as $U=\int dwg(w)n(w)w$, where U is the internal energy, $n(w)$ is the Bose population factor, and the integral is taken over the excitation bandwidth. The typical temperature of the $C(T)/T$ peak is roughly half the mode energy.[4] Applying this rule here, a peak in $g(w)$ is expected at $\hbar w_0\sim 13$ K. This estimate is consistent with the inelastic neutron-scattering results, which show a broad peak at $E=1.2$ meV ~ 13 K. This is not a simple single-ionlike excitation, as evidenced by the T^2 component of the heat capacity and the failure to model the magnetic-entropy-based upon various crystal-field schemes (which have broad features due to correlation effects). In-field specific-heat measurements [Fig. 6(b)] show that $C_{\mathrm{mag}}(T)$ becomes smaller and the T^2 behavior disappears with an applied field along the c axis. This is correlated with a gap opening in the spin-excitation spectrum as evidenced by the Q-integrated inelastic scattering data shown in Fig. 7. Information on this field-dependent gap is obtained from the NMR spin-lattice relaxation rates and from inelastic neutron scattering.

While the elastic neutron pattern at 0.035 K with a field of 9 T [Fig. 7(a)] reveals no extra peaks nor intensity differences compared to the zero-field pattern, showing that no long-range magnetic order is stabilized, significant diffuse scattering appears near $Q=0.78$ Å^{-1} [Fig. 9(a)] in a field of 9 T. The form of this diffuse scattering of a broad asymmetric peak (a sharp rise at low Q and a slow fall off toward high Q) is characteristic of 2D short-range order. The scattering from $Pr_3Ga_5SiO_{14}$ can be described analytically by a modified Warren function for 2D magnetic correlations.[25] The structure factor $P_{2\theta}$ around the peak is expressed by

$$P_{2\theta}=Km\frac{F_{hk}^2(1+\cos^2 2\theta)}{2(\sin\theta)^{3/2}}\left(\frac{L}{\sqrt{\pi}\lambda}\right)^{1/2}F(a)[J(z)]^2 \quad (1)$$

with

$$a=(2\sqrt{\pi}L/\lambda)(\sin\theta-\sin\theta_0) \quad (2)$$

and

$$F(a)=\int_0^{10}\exp[-(x^2-a)^2]dx. \quad (3)$$

L is the spin-spin-correlation length, λ is the wavelength, K is a scaling constant, m is the multiplicity of the reflection, F_{hk} is the two-dimensional structure factor for the spin array, and θ_0 is the center of the peak. The fits of the Q-integrated diffuse scattering to Eq. (1) [Fig. 9(b)] give a correlation length $L=25(1)$ Å and 29(1) Å for applied fields of 6 T and 9 T, respectively. This correlation length corresponds to 6 $\sim$7 in-plane kagome lattice spacings. The increasing L with increasing field shows that the short-range order or the nanoscale magnetic cluster size expands with increasing fields. The formation of these clusters coincides with the appearance of a spin gap in the excitation spectrum, the suppression of neutron-scattering inelastic spin excitations, and the gradual disappearance of the T^2 component of the specific heat in an applied field along the c axis.

To illustrate the low-dimensional nature of the diffuse scattering in applied fields, representative elastic scans within the $[H,K,0]$ plane are shown in Fig. 8. The central bank scans (using 0 T as a background) show diffuse scattering developing around the ferromagnetic points [1,0,0] and [0,1,0]. The upper and the lower banks of the instrument, which correspond to components of momentum transfer along the c direction, are shown in Fig. 8(a). Notice the significant diffuse scattering which persists out of the $[H,K,0]$ plane. The rodlike nature of the scattering is a key feature of 2D spin correlations. Integrating the total amount of diffuse scattering normalized to chemical Bragg peaks gives an upper limit of $0.08(3)\mu_B$/f.u. of Pr (assuming a ferromagnetic ordered moment within the spin cluster) at 9 T. This is significantly short of the full expected moment of $\sim 3\mu_B$ in a free-ion scenario, but a full moment is not expected due to the limited size of the clusters coexisting with paramagnetic spins. Neutron-scattering methods, being a bulk probe, are not sensitive to local inhomogeneous spin environments, but as a crude estimate, this puts a limit of only $\sim$3% of the sample being ordered within the clusters themselves.

The ^{69}Ga NMR relaxation-rate behavior with temperature provides detailed information on the Pr^{3+}-ion spin dynamics. Assuming that the spin-correlation function decays exponentially, the spin-lattice relaxation rate may be written as

$$1/T_1 = C_\perp\left(\frac{\tau_\perp}{1+\omega_I^2\tau_\perp^2}\right), \tag{4}$$

where $\tau_\perp$ is the transverse correlation time for electron spins and $C_\perp = \gamma_I^2\langle H_\perp^2\rangle$ is the square of the transverse component of the local field at a Ga site.[22,23] By summing over S spin neighbors i at a nuclear spin I, we have

$$\langle H_\perp^2\rangle = \frac{3}{2}\gamma^2\hbar^2 S(S+1)\sum_i \frac{1}{r_i^6}\sin^2\theta_i\cos^2\theta_i \tag{5}$$

with θ_i the angle between the connecting SI vector and the applied field for a paramagnetic system. Similarly we can write

$$1/T_2 = \frac{1}{2}C_\perp\left(\frac{\tau_\perp}{1+\omega_I^2\tau_\perp^2}\right) + C_\parallel\tau_\parallel \tag{6}$$

with $\tau_\parallel$ being the longitudinal correlation time, $C_\parallel = \gamma_I^2\langle H_\parallel^2\rangle$, $H_\parallel$ the z component of the local field and

$$\langle H_\parallel^2\rangle = \frac{1}{6}\gamma^2\hbar^2 S(S+1)\sum_i \frac{1}{r_i^6}S(S+1)(1-3\cos^2\theta_i). \tag{7}$$

The expression for $1/T_2$ holds provided $\tau_\parallel < 1/\Delta\omega$, where $\Delta\omega$ is the NMR linewidth of the selected spectral component. For $\tau_\parallel > 1/\Delta\omega$, $1/T_2$ is expected to saturate. The introduction of both transverse and longitudinal electron spin correlation times allows for the possibility of different mechanisms being of dominant importance for $\tau_\parallel$ and $\tau_\perp$, respectively. For spin-ordered systems, including frustrated AF with some degree of order in which the S spins may align along directions making an angle with the applied field, the angle θ_i should be modified to allow for the change in spin orientation. In addition, AF correlations of spins can result in a reduction in the fluctuating local field due to partial cancellation of dipolar fields at a Ga site.

A maximum in $1/T_1$ occurs for $\omega_I\tau_\perp = 1$ while for higher T, in the short-correlation-time case ($\omega_I\tau_\perp < 1$) the dipolar mechanism leads to $1/T_1 \sim C_\perp\tau_\perp$ and $1/T_2 \sim \frac{1}{2}C_\perp\tau_\perp + C_\parallel\tau_\parallel$. Inspection of Fig. 9 shows that for $T > 30$ K, the $1/T_1$ and $1/T_2$ curves lie close together suggesting that the fluctuating fields are isotropic with $\tau_\parallel = \tau_\perp$.

Values of $\tau_\perp$ obtained from the $1/T_1$ data as a function of T are shown in Fig. 13(a). We expect that the temperature dependence of the correlation time due to transitions between the ground state and low-energy excited states should be given by $\tau = \tau_0 e^{\Delta/T}$ with Δ the effective energy gap and the pre-exponential factor $\tau_0 \sim 10^{-11}$ s. This predicts that for $T < \Delta$ the correlation time for spin fluctuations will increase rapidly with decreasing T. Behavior of this kind has been found in μSR and Ga NQR relaxation-rate measurements in the quasi-2D AF $NiGa_2S_4$. We find that the Arrhenius expression is obeyed in $Pr_3Ga_5SiO_{14}$ for $T > 30$ K where the relaxation rates $1/T_2$ and $1/T_1$ coincide. The fit gives an energy gap $\Delta = 98$ K between the ground state and an excited singlet

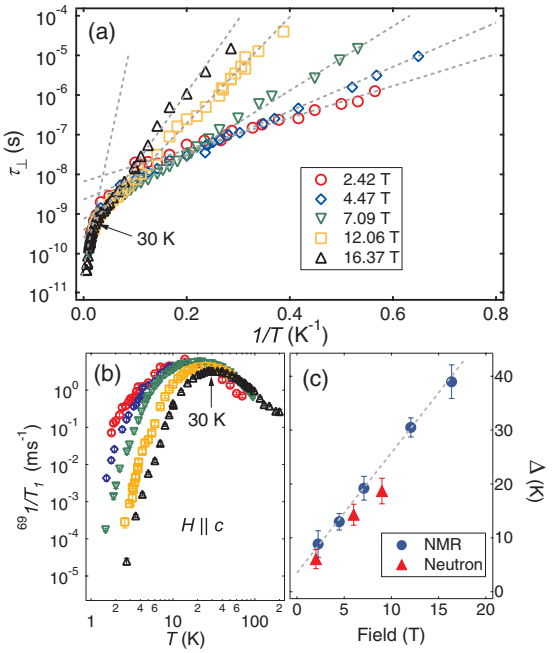

FIG. 13. (Color online) (a) Temperature dependence of the transverse spin correlation time $\tau_\perp$ at different fields extracted from $^{69}1/T_1$ vs T plot in (b). At $T > 30$ K, the gap $\Delta \approx 98$ K obtained from the slope is field independent. Below 30 K, the gap Δ_{NMR} has field dependence shown in (c) where the dashed line corresponds to the fit $\Delta_{NMR} = \Delta_0 + \alpha H$ with $\alpha = g\mu_B = 3.32\mu_B$ and $\Delta_0 = 3.5$ K. The field dependence of the spin gap in the excitation spectrum as derived from 0.035 K inelastic neutron-scattering results is shown for comparison.

state. However, relaxation-rate behavior for $T < 30$ K cannot be accounted for using the Arrhenius expression with a field-independent energy gap. Following a transition region below 30 K, over which the slope of the plot is continuously changing, the energy gap obtained from the slopes of the curves in the low-T region of Fig. 13(a), denoted Δ_{NMR}, is clearly field dependent with values plotted versus H as shown in Fig. 13(c). The fitted curve in this plot has the form $\Delta_{NMR} = \Delta_0 + \alpha H$, where the slope $\alpha \approx g\mu_B$ with μ_B the Bohr magneton and $g = 3.32$ close to the g value for the Pr^{3+} ion. The estimated zero-field gap obtained by extrapolating the low-temperature ($T < 30$ K) NMR relaxation data is, with a fairly large uncertainty, $\Delta_0 = 3.5$ K (see Fig. 11 caption). This value is much smaller than the high-T NMR value for Δ. We note that the integrated inelastic neutron-scattering data at 0.035 K give a field-dependent spin gap in the excitation spectrum very similar to the gap derived from the NMR correlation time behavior as shown in Fig. 13(c). This finding suggests that field-suppressed spin fluctuations are responsible for the field dependence in the inelastic neutron scattering. Other possible mechanisms such as field-induced small structural displacements will not lead to the observed behavior of the neutron-scattering or NMR relaxation rates with T and H.

It is important to attempt to distinguish CF-related excitations and collective kagome spin dynamics. For $T > 30$ K the NMR relaxation rates $1/T_1$ and $1/T_2$ converge as shown in Fig. 13 and it is clear that CF excitations are of dominant importance. The energy gap obtained from an Arrhenius fit to

the $1/T_1$ versus T data in this temperature range is consistent with the gap between the CF ground state and the second CF state used in the fit to the magnetic specific heat in Fig. 5. Between 10 and 30 K $1/T_1$ passes through a maximum and it is likely that CF excitations remain dominant with collective spin dynamics playing a minor role in the relaxation process. As T is lowered below 10 K collective spin excitations become increasingly important. This conclusion is based on the field-dependent gap behavior exhibited by both the NMR relaxation rate as a function of T in the range 2–10 K and the related spin-gap behavior in the neutron excitation spectrum.

While $1/T_1$ decreases at temperatures below the maximum shown in Fig. 12, $1/T_2$ continues to increase as T is lowered before exhibiting a field-dependent maximum below 7 K and then a dramatic decrease. The field-dependent behavior suggests field suppression of spin fluctuations. The reduction in spin fluctuations is attributed to the field-induced gap. In this picture spins will be increasingly confined to the lowest energy states as the temperature is lowered and/or the applied field is increased. Figure 13(c) shows that an applied field of 9 T corresponds to a gap of ~20 K.

The temperature dependence of $1/T_2$ is similar to that of $C_{\mathrm{mag}}(T)/T$ as seen in Fig. 12 (for $H=9$ T). This similarity in form is clearly associated with increasing occupation of the Pr^{3+}-ion ground state at low T. The NMR wipe-out effect which occurs when $1/T_2$ becomes less than a few microsecond can prevent detailed comparison of $C_{\mathrm{mag}}(T)/T$ with $1/T_2$ (Ref. 19) but in $Pr_3Ga_5SiO_{14}$ wipe-out does not occur and this allows the comparison to be made over a wide temperature range. Below 7 K, occupation of the ground state by the electron spins rapidly increases with decreasing T and both $1/T_2$ and C_{mag} drop to low values. The behavior of $1/T_2$ below 7 K may be accounted for by decrease in $\tau_{\parallel}$ and/or $H_{\parallel}$. While it is unlikely that $\tau_{\parallel}$ will shorten at low T, dynamic short-range transverse AF correlations of spins could result in a reduction in $H_{\parallel}$ leading to a change in the longitudinal low-frequency field contribution to $1/T_2$. If the spins tend to align perpendicular to the applied field this will result in changes in the angles θ_i in Eq. (7). In view of the uncertainties in the dynamical spin structure we have not attempted to model the relaxation process for $T<7$ K. We note that in this temperature range the NMR spectra show little further change in linewidth with decreasing T and the NMR shift is roughly constant (see Fig. 11).

The neutron-scattering results provide support for short-range transverse ordering of spins. The application of an external magnetic field perpendicular to the two-dimensional layers induces a gap in the spin excitation spectrum, but magnetic Bragg peaks indicative of ordering do not appear. There is only diffuse scattering present up to applied fields of 9 T which is modeled with the formation of nanoscale islands of ordered spins. This sort of ordering has been seen in other two-dimensional systems such as $NiGa_2S_4$,[26] but has only now been observed in a kagome lattice with applied fields.

Furthermore, the quadratic T dependence of C_{mag} for $H=0$ T and $T<4$ K suggests spin excitations in the system consistent with some form of spin ordering. The elastic neutron-scattering measurements for $T<1$ K provide strong evidence for 2D nanoscale ordering in the presence of an applied field. The neutron scattering gives a correlation length of 29 Å (~6–7 in-plane lattice spacings) for $H=9$ T. The NMR relaxation rate results suggest that at low temperatures the spin-correlation time $\tau_{\perp}$ is both H and T dependent as shown in Fig. 13(a). This is consistent with the suggestion, made above, that a field-dependent reduction in the c-axis component of the dipolar field at Ga sites could result from field-dependent short-range ordering leading to the anomalous behavior of $1/T_2$.

Recently, it has come to our attention that Zorko *et al.*[19] have published NQR and muon spin-relaxation experiments on $Pr_3Ga_5SiO_{14}$. They have postulated that the ground state is a possible magnetic singlet with experimental signatures that point toward Van Vleck paramagnetic behavior at low temperatures. We address these criticisms here before closing our paper. First, we do not exclude the possibility that the ground state could be a singlet. The specific-heat data have been fit with a singlet ground state in direct comparison to our model to show that this is a possibility. The nuclear component due to Pr complicates a clear determination of the electronic ground state.

The existence of a nonmagnetic singlet, if present, would have to be explained within the context of the numerous characterization methods detailed in this paper. First, the magnetic susceptibility would have a different form at low temperatures if the ground state was nonmagnetic. The upward curvature suggests that the ground state is magnetic. In addition, the heat capacity would not show a broad magnetic feature that is observed in our data with a T^2 dependence. Zorko *et al.*[19] argued that this is due to some sort of intrinsic disorder which creates a distribution of singlet levels that we are interpreting as a collective excitation. However, if this was the case, then it would be extremely unusual if the distribution would uniformly shift to higher energies as a function of applied fields. In addition, one would expect that the same sort of broad distribution of crystal fields would be present in $Nd_3Ga_5SiO_{14}$ (albeit with a series of doublets rather than singlets). Zorko *et al.* have shown that the local Ga environment in both compounds appears similar, implying that there is similar level of local disorder in both compounds. However, in the Nd case, there are sharp crystal-field excitations as shown by our previous work.[27] Therefore, there must be another reason for this broadness—it cannot be simply due to chemical disorder. Furthermore, we have shown through doping studies that by tuning the magnitude of the superexchange interaction J, the magnitude of the T^2 component can be systematically reduced in size to eventually induce some sort of spin freezing for weak exchange.[28] It would have to be a remarkable coincidence that such a behavior would be observed across a dozen different dopings in a concerted, consistent fashion if the heat-capacity anomaly was due to a broad distribution of singlets.

While we are not discrediting their work, it is clear that there are many inconsistencies that need to be resolved in order to determine the true nature of the ground state. We point out that muon spin-relaxation measurements have been shown in the past to alter crystal-field schemes in other Pr compounds.[29,30] Zorko *et al.* have dismissed this explanation based on the fact that the muon spin-relaxation and NQR measurements show similar relaxation at low temperatures,

but we point out that these probes are measuring different local environments. There is some ambiguity in determining the electronic ground state using these methods.

Finally, we point out in closing that singlet ground states in Pr systems have, in the past, shown unusual dynamic low-temperature states due to admixing with nearby crystal-field levels, as shown by recent work on compounds such as $PrAu_2Ge_2$.[31] While we cannot completely rule out that our ground state is not a singlet, we do emphasize that interesting physics can arise in these systems due to induced moments from applied fields and enhanced exchange interactions. Future measurements are clearly needed to unambiguously determine the full crystal-field scheme and elucidate the consequences of exchange and local electronic energy levels to the magnetism of this compound.

VII. CONCLUSION

In summary, in zero external field $Pr_3Ga_5SiO_{14}$ shows (i) no long-range magnetic ordering at temperatures down to 0.035 K, (ii) a T^2 dependence of the specific heat at low T, and (iii) spin excitations consistent with a highly degenerate state.[32] These findings place strong constraints on possible ground states. They are consistent with a dynamically disordered state with no conventional long-range magnetic order, such as observed in the triangular lattice $NiGa_2S_4$ (Ref. 26) and hyper-kagome $Na_4Ir_3O_8$.[33] However, the absence of magnetic diffuse scattering is unusual. One possibility is that the spins are truly dynamic on the neutron time scale. Note that the NMR correlation times given in Fig. 12 are determined in an applied field and somewhat shorter correlation times will apply in zero field.

The neutron-scattering results suggest that application of an external field parallel to the c axis leads to the formation of nanoscale magnetic clusters, whose size increases with H. This behavior is accompanied by reduction in the T^2 component of the specific heat and the opening of a spin gap in the excitation spectrum.[32] NMR relaxation rates provide information on the spin dynamics and confirm that a field-dependent gap can account for the dependence of the spin-correlation time on applied magnetic field for $T<30$ K. The NMR results are consistent with a dynamic ground state in which short-range spin correlations persist at temperatures well below 1 K. This dynamical state below 1 K may correspond to a spin-liquid state but future work is needed to establish this.

ACKNOWLEDGMENTS

This work was made possible by support through the NSF (Grants No. DMR-0084173 and No. DMR-0454672), the EIEG pro-gram (FSU), NSERC of Canada, and the state of Florida. The authors are grateful for the local support staff at the NIST Center for Neutron Research. Data analysis was completed with DAVE, which can be obtained at http://www.ncnr.nist.gov/dave/. We are grateful for useful discussions with P. Schlottmann and J. E. Greedan.

*ch.wiebe@uwinnipeg.ca

[1] H. T. Diep, *Magnetic Systems with Competing Interactions* (World Scientific, Singapore, 1994).
[2] A. P. Ramirez, in *Handbook of Magnetic Materials*, edited by K. H. J. Buschow (Elsevier, New York, 2001).
[3] J. S. Helton, K. Matan, M. P. Shores, E. A. Nytko, B. M. Bartlett, Y. Yoshida, Y. Takano, A. Suslov, Y. Qiu, J.-H. Chung, D. G. Nocera, and Y. S. Lee, Phys. Rev. Lett. **98**, 107204 (2007).
[4] A. P. Ramirez, B. Hessen, and M. Winklemann, Phys. Rev. Lett. **84**, 2957 (2000).
[5] A. S. Wills, A. Harrison, S. A. M. Mentink, T. E. Mason, and Z. Tun, Europhys. Lett. **42**, 325 (1998).
[6] C. Xu and J. E. Moore, Phys. Rev. B **76**, 104427 (2007).
[7] J. T. Chalker, P. C. W. Holdsworth, and E. F. Shender, Phys. Rev. Lett. **68**, 855 (1992).
[8] M. Siqueira, J. Nyéki, B. Cowan, and J. Saunders, Phys. Rev. Lett. **76**, 1884 (1996).
[9] G. Misguich, B. Bernu, C. Lhuillier, and C. Waldtmann, Phys. Rev. Lett. **81**, 1098 (1998).
[10] S. Yamashita, Y. Nakazawa, M. Oguni, Y. Oshima, H. Nojiri, Y. Shimizu, K. Miyagawa, and K. Kanoda, Nat. Phys. **4**, 459 (2008).
[11] Y. Kitaoka, T. Kobayashi, A. Ko-da, H. Wakabayashi, Y. Niino, H. Yamakage, S. Taguchi, K. Amaya, K. Yamaura, M. Takano, A. Hirano, and R. Kanno, J. Phys. Soc. Jpn. **67**, 3703 (1998).
[12] F. Vernay, K. Penc, P. Fazekas, and F. Mila, Phys. Rev. B **70**, 014428 (2004).
[13] R. Coldea, D. A. Tennant, and Z. Tylczynski, Phys. Rev. B **68**, 134424 (2003).
[14] H. Takeya, K. Ishida, K. Kitagawa, Y. Ihara, K. Onuma, Y. Maeno, Y. Nambu, S. Nakatsuji, D. E. MacLaughlin, A. Koda, and R. Kadono, Phys. Rev. B **77**, 054429 (2008).
[15] A. Yaouanc, P. Dalmas de Réotier, Y. Chapuis, C. Marin, G. Lapertot, A. Cervellino, and A. Amato, Phys. Rev. B **77**, 092403 (2008).
[16] C.-H. Chern, Phys. Rev. B **78**, 020403(R) (2008).
[17] P. Bordet, I. Gelard, K. Marty, A. Ibanez, J. Robert, V. Simonet, B. Canals, R. Ballou, and P. Lejay, J. Phys.: Condens. Matter **18**, 5147 (2006).
[18] J. Robert, V. Simonet, B. Canals, R. Ballou, P. Bordet, P. Lejay, and A. Stunault, Phys. Rev. Lett. **96**, 197205 (2006).
[19] A. Zorko, F. Bert, P. Mendels, P. Bordet, P. Lejay, and J. Robert, Phys. Rev. Lett. **100**, 147201 (2008); A. Zorko, F. Bert, P. Mendels, K. Marty, and P. Bordet, Phys. Rev. Lett. **104**, 057202 (2010).
[20] V. Simonet, R. Ballou, J. Robert, B. Canals, F. Hippert, P. Bordet, P. Lejay, P. Fouquet, J. Ollivier, and D. Braithwaite, Phys. Rev. Lett. **100**, 237204 (2008).
[21] J. E. Greedan, J. Mater. Chem. **11**, 37 (2001).
[22] C. P. Slichter, *Principles of Magnetic Resonance* (Springer, New York, 1989).
[23] A. Abragam, *Principles of Nuclear Magnetism* (Oxford Univer-

sity Press, England, 1961).
[24] X. S. Xu, T. V. Brinzari, S. McGill, H. D. Zhou, C. R. Wiebe, and J. L. Musfeldt, Phys. Rev. Lett. **103**, 267402 (2009).
[25] A. S. Wills, N. P. Raju, C. Morin, and J. E. Greedan, Chem. Mater. **11**, 1936 (1999).
[26] S. Nakatsuji, Y. Nambu, H. Tonomura, O. Sakai, S. Jonas, C. Broholm, H. Tsunetsugu, Y. Qiu, and Y. Maeno, Science **309**, 1697 (2005).
[27] H. D. Zhou, B. W. Vogt, J. A. Janik, Y. J. Jo, L. Balicas, Y. Qiu, J. R. D. Copley, J. S. Gardner, and C. R. Wiebe, Phys. Rev. Lett. **99**, 236401 (2007).
[28] H. D. Zhou, C. R. Wiebe, Y.-J. Jo, L. Balicas, R. R. Urbano, L. L. Lumata, J. S. Brooks, P. L. Kuhns, A. P. Reyes, Y. Qiu, J. R. D. Copley, and J. S. Gardner, Phys. Rev. Lett. **102**, 067203 (2009).
[29] R. Feyerherm, A. Amato, A. Grayevsky, F. N. Gygax, N. Kaplan, and A. Schenck, Z. Phys. B: Condens. Matter **99**, 3 (1995).
[30] T. Tashma, A. Amato, A. Grayevsky, F. N. Gygax, M. Pinkpank, A. Schenck, and N. Kaplan, Phys. Rev. B **56**, 9397 (1997).
[31] E. A. Goremychkin, R. Osborn, B. D. Rainford, R. T. Macaluso, D. T. Adroja, and M. Koza, Nat. Phys. **4**, 766 (2008).
[32] H. Tsunetsugu and M. Arikawa, J. Phys. Soc. Jpn. **75**, 083701 (2006).
[33] Y. Okamoto, M. Nohara, H. Aruga-Katori, and H. Takagi, Phys. Rev. Lett. **99**, 137207 (2007).